The Rho GTPase Wrch1 regulates osteoclast precursor adhesion and migration.

Hélène Brazier, Géraldine Pawlak, Virginie Vives, Anne Blangy

The Rho GTPase Wrch1 regulates osteoclast precursor adhesion and migration.

Hélène Brazier[a], Géraldine Pawlak[a,b], Virginie Vives[a] and Anne Blangy[a,*].

[a] Centre de Recherche de Biochimie Macromoléculaire, Montpellier University, CNRS, Montpellier, France

[b] INSERM U823, CNRS ERL3148 Université Joseph Fourier, Institut Albert Bonniot, Equipe DySAD, Site Santé, BP 170, F-38042 Grenoble cedex 9, France

[*] corresponding author:

anne.blangy@crbm.cnrs.fr

CRBM CNRS UMR 5237

1919 route de Mende

34293 Montpellier Cedex 5

FRANCE

Tel: +33 467 613 422

Fax: +33 467 521 559

Abstract.

An excess of osteoclastic bone resorption relative to osteoblastic bone formation results in progressive bone loss, characteristic of osteoporosis. Understanding the mechanisms of osteoclast differentiation is essential to develop novel therapeutic approaches to prevent and treat osteoporosis. We showed previously that Wrch1/RhoU is the only RhoGTPase whose expression is induced by RANKL during osteoclastogenesis. It associates with podosomes and the suppression of Wrch1 in osteoclast precursors leads to defective multinucleated cell formation. Here we further explore the functions of this RhoGTPase in osteoclasts, using RAW264.7 cells and bone marrow macrophages as osteoclast precursors. Suppression of Wrch1 did not prevent induction of classical osteoclastic markers such as NFATc1, Src, TRAP (Tartrate-Resistant Acid Phosphatase) or cathepsin K. ATP6v0d2 and DC-STAMP, which are essential for fusion, were also expressed normally. Similar to the effect of RANKL, we observed that Wrch1 expression increased osteoclast precursor aggregation and reduced their adhesion onto vitronectin but not onto fibronectin. We further found that Wrch1 could bind integrin ß3 cytoplasmic domain and interfered with adhesion-induced Pyk2 and paxillin phosphorylation. Wrch1 also acted as an inhibitor of M-CSF-induced prefusion osteoclast migration. In mature osteoclasts, high Wrch1 activity inhibited podosome belt formation. Nevertheless, it had no effect on mineralized matrix resorption. Our observations suggest that during osteoclastogenesis, Wrch1 potentially acts through the modulation of αvß3 signaling to regulate osteoclast precursor adhesion and migration and allow fusion. As an essential actor of osteoclast differentiation, the atypical RhoGTPase Wrch1/RhoU could be an interesting target for the development of novel antiresorptive drugs.

Key words.

Osteoclast, Podosome, Wrch1, Pyk2, Integrin

1. Introduction.

Bone resorbing osteoclasts are post-mitotic multinucleated cells formed after the fusion of monocyte/macrophage precursors (Boyle et al., 2003). Osteoclastic bone resorption involves the differentiation of progenitors into mononuclear prefusion osteoclasts (preOCs) that fuse to generate polykaryons, and the migration of osteoclasts towards the bone resorption site. Osteoclastic differentiation requires the two cytokines M-CSF (macrophage colony stimulating factor) and RANKL (receptor activator of NFκB-ligand) (Boyle et al., 2003). Osteoclast mediated bone resorption is tightly regulated at multiple levels, excessive osteoclast activity leading to progressive reduction of bone mass and modification of bone architecture that are associated with various diseases (Roodman, 2006, Teitelbaum and Ross, 2003). In particular osteoporosis which affects post menopausal women and older men has now become a major public health problem due to general population aging (Dennison et al., 2005).

Upon RANKL treatment, osteoclast precursors undergo profound changes. They exit the cell cycle (Ogasawara et al., 2004) while a complex transcriptional program is activated. RANKL induces the expression of NFATc1, a fundamental transcription factor in osteoclastogenesis (Takayanagi et al., 2002). RANKL also activates the expression of integrin ß3, ATP6v0d2 and DC-STAMP, which are essential for osteoclast precursor differentiation and fusion (Kim et al., 2008, Lee et al., 2006, McHugh et al., 2000, Miyamoto et al., 2000). Finally, increased expression of genes necessary for bone resorbing activity is also observed during osteoclastogenesis, including cathepsin K, TRAP and the tyrosine kinase Src.

Precursors kept in semi-solid culture medium, to prevent their anchorage to the substratum, are unable to differentiate into mature osteoclasts (Miyamoto et al., 2000); therefore adhesion-dependent signaling plays an important role during osteoclastogenesis. The major adhesion structures found in osteoclasts are podosomes. These structures are

formed by an F-actin core column whose orientation is perpendicular to the plasma membrane and to the extracellular matrix. The podosome core is surrounded by several adhesion molecules such as integrins, vinculin, talin and paxillin (Block et al., 2008, Saltel et al., 2008). Osteoclasts express integrins αvß3, α2ß1 and αvß1, integrin αvß3 being involved in most aspects of osteoclast biology. Integrin αvß3 is essential during osteoclast differentiation, most likely by controlling precursor migration and adhesion (Boissy et al., 1998, Kim et al., 2007, McHugh et al., 2000, Miyamoto et al., 2000). It is also necessary for osteoclast bone resorbing activity (Zou et al., 2007). Integrin αvß3 interaction with extracellular matrix proteins activates multiple signaling pathways, in particular phosphorylation cascades triggered by the tyrosine kinases Src and Pyk2 (Lakkakorpi et al., 2003, Miyazaki et al., 2004), to regulate podosome dynamics and organization, sealing zone formation and bone resorption (Destaing et al., 2008, Gil-Henn et al., 2007, Shyu et al., 2007). Much less is known about the importance of integrin signaling during osteoclast differentiation. Whereas integrin beta3 is essential for osteoclast differentiation, Src and Pyk2 are dispensable. Osteoclast precursors defective for Src or Pyk2 can differentiate into mature multinucleated osteoclasts, but they are defective for bone resorption (Gil-Henn et al., 2007, Sanjay et al., 2001). This suggests that the two kinases are not essential for differentiation although both where shown to regulate prefusion osteoclast spreading and migration (Duong et al., 2001, Lakkakorpi et al., 2003, Nakamura et al., 2001).

Osteoclast podosomes are highly dynamic and reorganize during osteoclast maturation and activity (Destaing et al., 2003). Individual podosomes are connected to their neighbors by F-actin cables. This allows podosome compaction to generate the different osteoclast specific superstructures: podosome clusters and rings in immature osteoclasts, the podosome belt at the periphery of mature osteoclasts and the sealing zone when they resorb bone mineralized matrix (Luxenburg et al., 2007). RhoGTPases are well known to control F-actin and adhesion

structure organization and then cell migration in various cell types (Burridge and Wennerberg, 2004, Cernuda-Morollon and Ridley, 2006). In osteoclasts, RhoA, Rac and Cdc42 are involved in the control of podosome assembly and organization, and in the regulation of adhesion signaling (Ory et al., 2008). So far, only Rac1 and 2 were shown to be necessary for osteoclast differentiation (Wang et al., 2008). To get a better view of the function of Rho GTPase signaling pathways in osteoclasts, we established the expression profile of RhoGTPases and their activators during RANKL-induced osteoclastogenesis. We found that among all RhoGTPases, only the expression of Wrch1 (Wnt1-Responsive Cdc42 Homolog 1)/RhoU was induced by RANKL. We also showed that suppression of Wrch1 expression in osteoclast precursors impaired fusion (Brazier et al., 2006). In the present studies, we further explored the roles of Wrch1 during osteoclast differentiation. We found that Wrch1 did not interfere with the overall transcriptional program induced by RANKL, in particular genes formerly reported as essential for precursor fusion were normally expressed. We previously showed that Wrch1 associated with adhesion structures: it localized to focal adhesion in fibroblasts and to podosomes in osteoclasts (Ory et al., 2007). We (Ory et al., 2007) and others (Chuang et al., 2007) also reported that Wrch1 regulated focal adhesion assembly and cell migration in fibroblasts and epithelial cells. Given these effects, we investigated how Wrch1 impacted on the adhesive and migration properties of osteoclast precursors. We present evidence that similar to RANKL, Wrch1 favors osteoclast precursor aggregation and diminishes their adhesion onto vitronectin. We also show that Wrch1 inhibits M-CSF-induced migration and integrin $\alpha v\beta 3$ downstream signaling of prefusion osteoclasts. Although we found that Wrch1 activity inhibited podosome belt formation, it did not affect sealing zone assembly and bone resorption in differentiated osteoclasts. Taking these findings together, we suggest that the RhoGTPase Wrch1 has an essential function during

osteoclastogenesis by regulating cell adhesion and migration, potentially through the modulation of integrin αvß3 downstream signaling.

2. Materials and Methods

2.1 Antibodies, reagents, plasmid and retroviral constructs.

Vitronectin was from R&D System, fibronectin was from SIGMA, anti-paxillin and -Pyk2 phosphospecific antibodies were from Biosource, and anti-phospho-ERK1/2 and anti-Gapdh were from Cell Signaling Technology, anti-ERK was from Santa Cruz, anti-Pyk2 and anti-paxillin were from Transduction Laboratories. Anti-ß actin and anti-vinculin antibodies, bisbenzimide Hoechst dye and TRITC labeled-Phalloidin were from Sigma, Alexa 350-conjugated Phalloidin was from Invitrogen. Retroviral pMXs and plasmid pEGFP constructs to express GFP and GFP-fused wild type, active Q107L and inactive T63N Wrch1 mutants as well as Luciferase and Wrch1 shRNA retroviral pSIREN expression vectors were described elsewhere (Brazier et al., 2006, Ory et al., 2007). The pGEX vector expressing integrin ß3 cytoplasmic domain (Zhang and Hemler, 1999) was a generous gift from C. Albiges-Rizo (Grenoble, France). Specific anti Wrch1 antibodies were obtained by rabbit injection with a mixture of two mouse Wrch1 C-terminal sequence peptides coupled to tyroglobulin: CQHSDSQLQPKKSKSR and TPDKVRDLSKSWWRKYC. Antibodies were then affinity purified on the same peptides coupled to bovine serum albumin.

2.2 Cell culture

293T and RAW264.7 cells were cultured in a humidified incubator at 37 °C and 5 % CO2, in growth medium (GM): DMEM or alpha-MEM respectively, supplemented with 10 % fetal calf serum and 2 mM glutamine. For osteoclast differentiation, RAW264.7 cells were transferred to differentiation medium, i.e. GM supplemented with 25 ng/mL RANKL (Peprotech). Medium was changed every other day. Fusion occurred after 3 to 4 days. Prefusion RAW264.7 cells treated for 72 hours with RANKL were used as preosteoclasts (pOCs). Bone marrow macrophages (BMMs) were prepared from bone marrow of 4-to 6-

week-old C57BL/6 mice, in a humidified incubator at 37 °C and 5 % CO2. Non adherent bone marrow cells were grown for 24 hours in GM supplemented with 30 ng/mL M-CSF (Peprotech) as described (Brazier et al., 2006). BMMs were then kept in GM supplemented with 30 ng/mL M-CSF or transferred for three days into differentiation medium i.e. GM supplemented with 30 ng/mL M-CSF and 100 ng/mL RANKL, to obtain prefusion osteoclasts.

2.3 Retrovirus production and cell infection

Retroviral particles production and RAW264.7 cell infections were performed as described previously (Brazier et al., 2006, Ory et al., 2007). Briefly retroviral particles were produced from HEK293T cells transfected with the Friend MLV Gag-Pol and VSV-G expression vectors and with a pMXs vector expressing GFP-fused wild type or active Q107L Wrch1 (Brazier et al., 2006, Ory et al., 2007) or with a pSiren-RetroQ vector (BD Biosciences Clontech) expressing short hairpin RNA targeting either firefly luciferase or Wrch1 GTPase (Brazier et al., 2006). After incubation with retroviruses, RAW 264.7 cells were selected for infection using 3µg/mL puromycin. For BMM infection, 10^7 non adherent bone marrow cells were grown in a 60 mm dish for 24 hours in GM supplemented with 30 ng/mL M-CSF. Adherent cells were then infected as above. After 24 hour recovery in GM supplemented with 30 ng/mL M-CSF, infected cells were selected by addition of puromycin (2 µg/mL) for another 48 hours.

2.4 Cell proliferation assay

10^4 RAW264.7 cells were seeded in 12-well plates. At desired time points, cells were fixed with formalin 3.7% in PBS for 10 min and stained with 0.1% crystal violet for 30 min. After extensive washing with water to remove excess stain, cells were lysed in 10% acetic

acid and the OD595 was measured. Absorbance was converted in cell number according to standard wells containing known numbers of RAW264.7 cells.

2.5 Transwell migration assay

Migration assays were performed in 24-well plates using 8µm pore HTS FluoroBlok inserts (Falcon). Undifferentiated RAW264.7 cells or preosteoclasts were scraped in growth or differentiation medium respectively. 5000 cells were seeded in the upper chamber of the transwell devices. Lower chamber contained the appropriate growth or differentiation medium with or without 50 ng/ml M-CSF (Peprotech). For BMMs or BMM derived pOCs, prior to the assay cells were scraped and transferred for 1 hour in GM containing 10 ng/mL M-CSF and supplemented with 100 ng/mL RANKL in the case of preOCLs. 5000 cells were then seeded in the upper chamber of the transwell devices. Lower chamber contained GM with 10 or 60 ng/mL M-CSF, supplemented with 100 ng/mL RANKL in the case of preOCLs. Each point was performed in duplicate. After 24 hours, cells were fixed with formalin 3.7% in PBS for 15 minutes and labeled with propidium iodine (Sigma). The entire lower face of the membrane was imaged under an inverted LEICA DMIRE2 microscope using a 10x PL Fluotar (NA=0.3) phase objective. Images were captured with a CCD micromax 1300 Y/HS camera (Roper Scientific Princeton Instruments) controlled by MetaMorph 7.0 software (Molecular Devices). The cells were then automatically counted with an image J derived software developed by Montpellier RIO Imaging (http://www.mri.cnrs.fr/index.php?m=38).

2.6 Cell aggregation, spreading and adhesion assays

For aggregation assays, RAW264.7 cells were scraped in calcium- and magnesium-free PBS, washed and resuspended in 10mM Hepes-buffered (pH 7.4) calcium- and magnesium-free PBS containing 5mM EDTA or 2mM CaCl2. $2x10^5$ cells were seeded in 12-well plates

coated with 4% BSA and incubated at 37°C on a gyratory shaker for 15 min at 70 rpm. Cell aggregation was followed under phase contrast using an inverted microscope (Leica DMIRB) and photographs were taken with a CCD camera (Hamamatsu Photonics) controlled by Hi.Pic software (Hamamatsu).

For spreading assays, 10^5 RAW264.7 cells were grown for two days in 60-mm plates. Two random microscopic fields per plate were captured for analyzes, using a Leica DMIRB inverted microscope equipped with a CDD camera (Hamamatsu Photonics). Spread cells were defined as cells with extended processes, lacking a rounded morphology and not phase-bright whereas non-spread cells were defined as rounded and phase-bright under microscope.

Adhesion assays were performed in 96 well plates coated overnight at 4°C with 1 to 20 µg/ml vitronectin or fibronectin, then saturated with 1% BSA in PBS. RAW264.7 or bone marrow derived cells were scraped, washed and resuspended in serum-free alpha-MEM and seeded at 10^5 cells per well. Each point was performed in triplicate. After 30 min of incubation at 37°C unattached cells were washed away with PBS and adherent cells were quantified as in the proliferation assays. To calculate the percentage of adhered cells, the OD595 was determined in triplicate wells and reported to the OD595 measured in wells in which all 10^5 cells were stained.

2.7 Adhesion-induced signaling.

RAW264.7 cells were scraped and washed twice in alpha-MEM containing 10mM Hepes-buffered (pH7.4) and 0.1% BSA and then kept in suspension for 2 hours at 37°C. Equal numbers of cells were then lysed immediately or replated onto 5 µg/ml vitronectin coated dishes and kept at 37°C. At desired time points, unattached cells were washed away with ice-cold PBS and the remaining cells were scraped in lysis buffer (50 mM Tris pH7.4, 150 mM NaCl, 1% Igepal, 10% glycerol, 1mM Na3VO4 and protease inhibitor cocktail

(Sigma)). Lysates were clarified by centrifugation (16,000xg, 15 min at 4°C) and protein concentrations were measured by bicinchoninic acid protein assay (Biorad). Equal amounts of proteins were then analyzed by western blot.

2.8 Indirect immunofluorescence and resorption assays on osteoclasts.

To determine podosome organization, osteoclasts were scraped from plastic culture dishes after 5 days in differentiation medium, seeded on glass coverslips and incubated for another 48 hours in differentiation medium. Cells were fixed with formalin 3.7% in PBS for 15 minutes and permeabilized with 0.1% Triton X-100 in PBS for 1 min. Actin was stained using rhodamine-labeled phalloidin and nuclei with Hoechst-33258 dye (Sigma). Osteoclasts were mounted in Mowiol 40-88 (Sigma) and their podosome organization was assessed under an upright Zeiss AxioImager microscope using a 10x Plan Neofluar (NA=0.3) objective (Zeiss).

For immunofluorescence, osteoclasts obtained as above were seeded on Osteologic calcium phosphate coated coverslips (BD Biocoat) in differentiation medium for 48 hours, fixed, permeabilized and actin was stained as above. Immunofluorescence was performed as described previously (Ory et al., 2007) using mouse monoclonal anti-vinculin antibody revealed with Alexa Fluor 546-conjugated secondary antibody (Invitrogen). Cells were mounted as above and observed under an upright Zeiss Axioimager microscope using a 63x Plan-APOCHROMAT (NA=1.4) oil objective (Zeiss). Z-stacks (steps of 300 nm) of images were captured with CoolSnap HQ2 CCD camera (Photometrics) controlled by MetaMorph 7.0 software (Molecular Devices). Images were deconvolved using the Maximum Likelihood Estimation algorithm and Huygens software (Scientific Volume Imaging).

For resorption assays, osteoclasts were seeded in Osteologic 16-well slides (BD BioCoat) for 48 hours, fixed and labeled for actin and nuclei as above. To count

multinucleated cells, slides were mounted in 20mM Tris pH 7.5 in 80% glycerol and entire wells were imaged using the same devices as for transwell assays. Multinucleated cells were manually counted on those images. Slides were then stained by Von Kossa as described (Contractor et al., 2005). Briefly, slides were incubated in 5% sodium hyperchlorite for 5 minutes to dislodge osteoclasts, washed with water, exposed under UVC (254nm) for 45 minutes in 5% silver nitrate (Sigma), then developed for 30 seconds with 5% sodium carbonate (Sigma) in 25% formalin and finally fixed with 5% sodium thiosulfate (Sigma) for 2 minutes. Slides were scanned as above and the resorbed areas were measured using MetaMorph 7.0.

2.9 *Real-time PCR analyses*

Real time PCR analyses were performed as described earlier (Brazier et al., 2006). Primers used to amplify Wrch1, Gapdh, Src and TRAP were the same as in (Brazier et al., 2006) and the primers used to amplify NFATc1, ATP6v0d2 and DC-STAMP were those described in (Kim et al., 2008). For integrin ß3 we used 5'-GGCCTTCGTGGACAAGCCTG-3' and 5'-CGGGACACCTGGTCGGTTAG-3' and for Cathepsin K 5'-TGGAGGCCTCTCTTGGTGTC-3' and 5'-CCACAAGATTCTGGGGACTC-3', as upstream and downstream primers respectively.

2.10 Pull down assays.

Expression of GST or GST-fused integrin ß3 cytoplasmic domain was induced in exponentially growing BL21 *E. coli* strain by addition of 1 mM IPTG for 4 hours. Bacteria lysates were prepared by sonication in PBS, clarified and GST proteins were bound to glutathione-conjugated Sepharose beads (GE Healthcare). HEK293T cells were transiently transfected for 24 hours with pEGFP expression vectors for GFP or GFP-fused Wrch1 wild

type or Q107L using JetPEI according to manufacturer's instructions (Qiagen). RAW264.7 cells were transduced with retroviruses expressing GFP or GFP-fused Wrch1 Q107L as described above. HEK293T and RAW264.7 cells were lysed for 30 minutes in lysis buffer (20 mM Tris pH8, 137 mM NaCl, 1% Igepal, 10% glycerol, 1mM Na3VO4, 10 mM NaF and protease inhibitor cocktail (Sigma)). After clarification by centrifugation, lysates were incubated for two hours with 30 µg of GST fusion proteins bound on sepharose beads. After extensive washing in lysis buffer and PBS, proteins bound to beads were analyzed by western blot.

3. Results

3.1. Wrch1 is not essential for the establishment of osteoclastogenesis transcriptional program.

We reported earlier that Wrch1 mRNA expression increased dramatically during RANKL-induced osteoclastogenesis and that it is essential for osteoclast differentiation (Brazier et al., 2006). We generated and purified polyclonal antibodies against the C-terminal hypervariable region of mouse Wrch1 (aminoacids 242 to 258). In RAW264.7 cells, the antibodies detected a 27 kD protein, compatible with the calculated molecular weight of Wrch1. The intensity of the signal increased during RANKL-induced osteoclastogenesis (Fig 1A and 1B) and disappeared in cells expressing Wrch1 specific shRNAs (Fig 1C). Thereby we showed that in agreement with the induction of its mRNA, Wrch1 protein expression increased during RANKL-stimulated osteoclastogenesis.

Wrch1 is essential for early osteoclast differentiation, suppression of Wrch1 expression resulting in severe reduction of fusion index (Brazier et al., 2006). We performed quantitative PCR analyses to identify genes which induction by RANKL could be defective in the absence of Wrch1. We found a normal expression of all characteristic markers of osteoclastic differentiation such as NFATc1, Src, TRAP and Cathepsin K (Fig 1D). Expression of genes shown to be essential for preosteoclast fusion was also normal: integrin ß3, ATP6v0d2, DC-STAMP (Fig 1D), MFR or ADAM8 (not shown).

Osteoclastic differentiation stimulated by RANKL requires osteoclast precursors to exit the cell cycle (Ogasawara et al., 2004). To test whether Wrch1 could be involved in this process, we analyzed the effect of Wrch1 overexpression on undifferentiated RAW264.7 cell growth. We found that cells expressing GFP-fused Wrch1 wild type (WT) or active (Q107L) presented a similar growth rate as compared to GFP-expressing cells (Fig 1E).

These observations suggest that Wrch1 essential role during osteoclastogenesis is not through the control of gene transcription or RANKL-induced cell cycle exit of precursors.

3.2. Wrch1 affects preosteoclast adhesion and Pyk2 phosphorylation in response to integrin engagement.

Wrch1 was shown to localize to osteoclast adhesion structures and to control fibroblast adhesion to the substratum (Chuang et al., 2007, Ory et al., 2007). As integrin ß3 mediated anchorage is essential for osteoclast differentiation (Miyamoto et al., 2000), we tested whether Wrch1 was involved in the control of preOC adhesion.

We observed that after 3 days of RANKL treatment, preOC grew as aggregates as compared to undifferentiated RAW264.7 cells (Fig 2A). We observed that undifferentiated RAW264.7 cells expressing Wrch1-Q107L, and to a lesser extent Wrch1-WT, also grew as aggregates (Fig 2A). It suggested that Wrch1 expression could favor cell-cell contacts during osteoclastogenesis. To confirm this, we performed cell aggregation assays in suspension. RAW264.7 cells were dissociated and then left in suspension in the presence of calcium to allow cell-cell contact reformation. We observed that preOC formed aggregates much more efficiently than undifferentiated cells (Fig 2B). In these cells, we found that expression of Wrch1-WT or Q107L favored aggregate formation (Fig 2B). This suggests that Wrch1 expression during osteoclastogenesis participates in osteoclast precursor aggregation induced by RANKL. We also observed that undifferentiated RAW264.7 cells expressing Wrch1 exhibited a spreading defect compared to GFP-expressing cells (Fig 2C), suggesting the GTPase may also affect adhesion to the substratum, an integrin-dependent process.

To confirm this observation, we performed adhesion assays onto plates coated with vitronectin or with fibronectin. We observed that RANKL treatment reduced the capacity of RAW264.7 cell to adhere onto vitronectin (Fig 3A) whereas it increased adhesion onto

fibronectin (Fig 3B). Similarly, adhesion capacity of undifferentiated RAW264.7 cells onto vitronectin was reduced upon Wrch1-WT or Wrch1-Q107L expression (Fig 3A), whereas adhesion onto fibronectin was not affected (Fig 3B). Importantly, we found that Wrch1-Q107L expression and RANKL treatment also reduced BMMs adhesion to vitronectin (Fig 3C).

As it modulates adhesion onto vitronectin, we tested Wrch1 effects on adhesion-dependent signaling downstream of αvß3. Consistent with previous reports, upon adhesion of GFP-expressing RAW264.7 cells onto vitronectin, we observed a strong induction of Pyk2 autophosphorylation on Y402 and of the downstream phosphorylation of paxillin on Y31 and Y118 (Fig 3D). Expression of active Wrch1 strongly inhibited the phosphorylation of Pyk2 Y402 and paxillin Y31, while paxillin Y118 phosphorylation was less affected. Conversely, we did not observe any defect in adhesion-induced ERK phosphorylation. These results show that the GTPase Wrch1 can interfere with part of αvß3 integrin downstream signaling induced by adhesion.

Wrch1 associates with adhesion structures (Ory et al., 2007) and affects αvß3 integrin signaling. We performed GST pull down experiments to test if the GTPase could bind integrin ß3 cytoplasmic domain. We observed that GFP-fused Wrch1 wild type and Q107L mutant expressed in HEK293T cells bound efficiently to integrin ß3 (stars in Fig 3E). Consistently, we found that Wrch1-Q107L could bind to integrin ß3 cytoplasmic domain when expressed in RAW264.7 cells, as endogenous Pyk2 did (stars in Fig 3F).

Taken together, these observations suggest that the induction of Wrch1 by RANKL participates in the modification of cell-cell and cell-substratum adhesion properties of cells undergoing osteoclastogenesis. They also suggest Wrch1 could potentially act through αvß3, the major integrin in osteoclasts.

3.3 Wrch1 inhibits preosteoclast chemotactic migration.

Since Pyk2 Y402 phosphorylation was shown to be essential to stimulate preOC migration toward M-CSF (Lakkakorpi et al., 2003), we then tested if Wrch1 could regulate this process. We performed transwell assays using RAW264.7 cells expressing GFP and treated (preOCs) or not (undifferentiated) with RANKL for three days. We observed that both undifferentiated cells (white bars) and preOCs (grey bars) exhibited a low rate of spontaneous migration (-MCSF, Fig 4A). Less than 10% of the cells had migrated to the lower chamber after 24 hours. In these conditions, expression of Wrch1-WT or -Q107L did not affect cell migration (-MCSF, Fig 4A).

Addition of M-CSF to the lower chamber (+MCSF, Fig4A) strongly stimulated preOCs migration (grey bars) whereas undifferentiated RAW264.7 cell migration was only slightly affected (white bars). Interestingly, we observed that Wrch1 overexpression in preOCs strongly inhibited M-CSF-induced chemotactic migration (grey bars +MCSF, Fig4A) whereas it was of little effect in undifferentiated cells (white bars +MCSF, Fig4A).

Similarly, we observed that undifferentiated BMMs exibited a low rate of spontaneous migration and did not respond to M-CSF (Fig4B, white bars). In these conditions, expression of Wrch1-Q107L had no effect on BMM migration. As with RAW264.7 cells, we found that addition of M-CSF to the lower chamber stimulated GFP-expressing BMM-derived preOCs migration. Finally, expression of GFP-Wrch1-Q107L in preOCs abolished the chemoattractant effect of M-CSF (Fig4B, grey bars).

Taken together, these observations suggested that Wrch1 could act as a negative regulator of preosteoclast migration. To confirm this, we tested the effect of Wrch1 shRNA expression on the migration of preosteoclasts. We observed that suppression of Wrch1 did not modify the spontaneous migration of preOCs (black bars, Fig 4C) but it strongly increased M-

CSF-activated preOC migration (hatched bars, Fig 4C). Induction of Wrch1 expression and efficient silencing by shRNAs were assessed by western blot (Fig 4D).

These results show that Wrch1 is a negative modulator of preOC migration in response to M-CSF.

3.4 Wrch1 activity influences podosome organization but not resorption.

Wrch1 activity interferes with αvß3-mediated adhesion signaling in preOCs, in particular by inhibiting Pyk2 Y402 autophosphorylation. Pyk2 was reported to be essential for correct podosome belt and sealing zone organization in osteoclasts and for bone resorbing activity (Gil-Henn et al., 2007). We previously found that Wrch1-Q107L and to a lesser extent Wrch1-WT associated with osteoclast podosome belt (Ory et al., 2007). We thus tested whether Wrch1 could affect podosome patterning in osteoclasts. In about 70% of control osteoclasts expressing GFP, podosomes organized as a peripheral belt (Fig 5A), which corresponds to normal podosome organization in mature osteoclasts (Destaing et al., 2003). Interestingly, in 70% of osteoclasts expressing Wrch1-WT or -Q107L podosomes rather organized as rings or clusters (Fig 5A). Podosome organization was similar in osteoclasts expressing GFP and GFP-fused Wrch1-T63N inactive mutant. These obervations suggest that Wrch1 activity can influence podosome organization.

We then seeded the osteoclasts on mineralized matrices to induce the assembly of the sealing zone. We found that Wrch1-Q107L, and less efficiently Wrch1-WT, associated with the sealing zone, whereas Wrch1-T63N did not (Fig 5B). Nevertheless, we did not find any defect of sealing zone assembly in osteoclasts overexpressing Wrch1-WT, Q107L or T63N (not shown). Consistently, when we measured mineralized matrix resorption, we did not

observe any difference in between control osteoclasts and those expressing Wrch1-WT, Q107L or T63N (Fig 5C).

These observations suggest that despite its effect on podosome belt organization, Wrch1 does not affect sealing zone formation and bone resorption.

4. **Discussion**

Our earlier studies identified the RhoGTPase Wrch1 as essential for osteoclast precursor fusion (Brazier et al., 2006). We now show that suppression of Wrch1 does not interfere with the overall transcriptional program induced by RANKL during osteoclastogenesis. In particular, the essential transcription factor NFATc1 is induced normally and later osteoclastic markers such as TRAP and cathepsin K are expressed. More interestingly, we did not observe any defect in the expression of genes shown to be essential for osteoclast differentiation and fusion such as DC-STAMP, ATP6v0d2 or integrin ß3. Therefore, the role of Wrch1 during early osteoclastogenesis does not appear to be through the regulation of transcription, although we cannot exclude that suppression of the GTPase interferes with the expression of as yet unidentified genes essential for osteoclast fusion. The analysis of the transcriptome of Wrch1-deficient cells during differentiation may lead to the identification of novel essential actors for osteoclastogenesis.

Wrch1 is an atypical RhoGTPase: it exhibits rapid intrinsic nucleotide exchange rate and the activity of ectopically expressed wild type Wrch1 is comparable to that of the active Q107L mutant (Shutes et al., 2004). Consistently, in RAW264.7 cells we found that wild type Wrch1 had attenuated but similar effects as compared to active Wrch1-Q107L. We had made similar observations in HeLa and NIH3T3 cells (Ory et al., 2007). In those studies, we also showed that Wrch1-T63N inactive mutant had no effect on NIH3T3 cell adhesion and migration, contrarily to Wrch1 shRNAs (Ory et al., 2007). The T63N mutation of Wrch1 leads to a nucleotide free GTPase unable to bind effectors and activate downstream signaling, the equivalent of the T17N mutant of Rac or the T19N mutant of RhoA for instance (Saras et al., 2004). Unlike Wrch1 wild type and Q107L active mutant, Wrch1-T63N did not associate with osteoclast podosomes or with focal adhesions in fibroblasts and epithelial cells (Ory et

al., 2007) and it did not associate with the sealing zone (this study). Expression of Wrch1-T63N had no incidence on the differentiation of RAW264.7 cells into osteoclast, contrarily to Wrch1 shRNAs (Brazier et al., 2006), and it did not perturb mineralized matrix resorption. Therefore, we could not use Wrch1-T63N as a dominant negative to inhibit the activity of the endogenous GTPase in osteoclasts, unlike what was done using Rac1-T17N or RhoA-T19N for example (Ory et al., 2000).

In epithelial HeLa cells, Wrch1 was shown to participate in the regulation of multiple signaling pathways including Myosin light chain phosphorylation, activation of PAK (p21 Activated Kinase), Jun kinase and Akt (Chuang et al., 2007), suggesting it can exert pleiotropic regulatory functions. We report here that Wrch1 can inhibit M-CSF-induced migration of preOCs derived either from RAW264.7 cells or from bone marrow macrophages. On the contrary, we found previously that it activated fibroblast migration in response to serum (Ory et al., 2007). Wrch1 was also reported to regulate positively epithelial cell migration in response to wound healing (Chuang et al., 2007). This suggests that through the control of multiple signaling pathways, Wrch1 can drive differential effects depending on the cell type. Here we also present data suggesting Wrch1 negatively regulates Pyk2 phosphorylation in preOCLs. Conversely, in HEK293 cells ectopic Pyk2 phosphorylation was increased by co-expression of wild type Wrch1 or of active Q107L mutant (Ruusala and Aspenstrom, 2008). This again suggests Wrch1 can participate in modulating various intracellular signaling cascades that will lead to adverse effects depending on the physiological system.

We found that Wrch1 colocalized with vinculin, surrounding the actin core of isolated podosomes or lining the podosome belt (Ory et al., 2007) and the sealing zone (this work) as a double ring. In HeLa cells, Wrch1 was recruited to Src-induced podosomes only when they were also associated with vinculin (Ory et al., 2007). Vinculin is an essential regulator of

focal adhesions (Humphries et al., 2007): it increases focal adhesion number and favors their maturation. On the contrary, we reported earlier that Wrch1 reduced focal adhesion number and inhibited their maturation (Ory et al., 2007). In osteoclasts, vinculin recruitment increases around osteoclast podosomes while they progressively organize as rings and belts (Luxenburg et al., 2006). As opposed to this, we show here that increasing Wrch1 activity perturbed podosome belt formation. These observations suggest that Wrch1 could be a counterpart for the stabilizing action of vinculin to allow the dynamics of adhesion structures. In particular, Wrch1 may participate with vinculin to the control of podosomes dynamics during osteoclast differentiation. Unfortunately, no information is available so far about the dynamics and the role of podosomes during early osteoclastogenesis and the function of vinculin in this process and in bone resorption is not known.

Wrch1 associates with podosomes and focal adhesions (Ory et al., 2007). The GTPase was shown to regulate migration and focal adhesion assembly in fibroblast and epithelial cell systems (Chuang et al., 2007, Ory et al., 2007). Here we show that Wrch1 can also regulate osteoclast precursor adhesion and migration. Interestingly, the effects of Wrch1 expression in osteoclast precursors were similar to those observed when we treated them with RANKL. Wrch1 expression or RANKL treatment both increased RAW264.7 cell aggregation. In RAW264.7 cells and in BMMs, Wrch1 expression decreased their adhesion onto vitronectin, similar to RANKL treatment. Therefore, Wrch1 induction by RANKL could participate in the modification of cell adhesive properties that we found to occur upon osteoclast differentiation. It was shown that adhesion conditions highly influence osteoclast precursor fusion. Multinucleation does not occur if cells undergo differentiation in liquid or semisolid substrate conditions, although cells can commit to the osteoclast lineage, as shown by normal induction of differentiation markers (Miyamoto et al., 2000). Similarly, in the absence of Wrch1, fusion does not occur in a context where all osteoclast differentiation markers tested

are expressed correctly. In line with our observation that Wrch1 and RANKL can promote rounding and aggregation of RAW264.7 osteoclast precursors, an early report mentioned that during osteoclastogenesis induced by 1,25-dihydroxyvitamin D3, chicken monocytes rounded up and formed aggregates (Boissy et al., 1998). During this process, integrin ß3 expression was induced, it translocated to the cell surface and accumulated in the region of cell-cell contact. Finally a peptide blocking integrin αvß3 function inhibited osteoclast precursor fusion (Boissy et al., 1998). Regulation of integrin αvß3 activity by endocytic recycling is known to impact on cell adhesion and migration but also receptor tyrosine kinase signaling (Caswell and Norman, 2008). We show that Wrch1 interferes with adhesion-induced alphaVbeta3 signaling by inhibiting Pyk2 and paxillin phosphorylation. Through its interaction with the cytoplasmic domain of integrin ß3, Wrch1 may control integrin αvß3 trafficking to influence osteoclast precursor adhesion and migration as well as intracellular signaling. To challenge this hypothesis, detailed study of the dynamics of integrin αvß3 localization during RANKL-induced osteoclastogenesis would be needed.

Despite it was established that integrin ß3 has an essential role for osteoclast differentiation and is selectively required for fusion (Faccio et al., 2003, McHugh et al., 2000, Miyamoto et al., 2000), little is known about its actual function. The overall mechanisms that control osteoclast precursor adhesion and migration during osteoclastogenesis still remains poorly documented. The dynamic regulation of integrin signaling is essential to ensure the turnover of adhesion contacts for efficient cell adhesion and migration (Webb et al., 2004). For instance, impairing paxillin phosphorylation leads to defects in both the formation of focal adhesion and the disassembly of adhesion structures (Deakin and Turner, 2008, Webb et al., 2002). We observed that Wrch1 decreased osteoclast precursor adhesion onto vitronectin, bound to integrin ß3 cytoplasmic domain and hindered adhesion-induced integrin αvß3 signaling by inhibiting paxillin and Pyk2 phosphorylation in response to adhesion onto

vitronectin. Therefore, Wrch1 appears as an important regulator of αvß3 integrin signaling. Expression of Pyk2 Y402F mutant or antisense RNAs was reported to inhibit osteoclast migration in response to M-CSF and their spreading onto vitronectin (Duong et al., 2001, Lakkakorpi et al., 2003). Consistently, we found that Wrch1 interfered with Pyk2 Y402 phosphorylation and inhibited adhesion to vitronectin and migration in response to M-CSF. Nevertheless, precursors derived from Pyk2-/- mice can still form multinucleated cells (Gil-Henn et al., 2007) whereas Wrch1 is essential for preOC fusion (Brazier et al., 2006). This suggests that Wrch1 regulates other essential pathways during early osteoclastogenesis. Integrin ß3-/- preosteoclasts are deficient for adhesion-induced ERK activation and high doses of M-CSF, which activate c-Fms and restore ERK phosphorylation, can rescue differentiation of ß3-/- osteoclasts (Faccio et al., 2003). This highlights a prominent role of the ERK pathway during osteoclastogenesis. Nevertheless, we did not observe any effect of Wrch1 on ERK phosphorylation, consistent with our observations in fibroblasts (not shown) and another report in HeLa cells (Chuang et al., 2007).

We found that increased Wrch1 activity led to impaired podosome belt formation in osteoclasts derived from RAW264.7 cells. Nevertheless, this did not correlate with defects in sealing zone formation and mineralized matrix resorption. Only mineralized matrices can induce the formation a sealing zone, most likely through the activation of osteoclast receptors that still remain unknown (Jurdic et al., 2006). Podosome density is much higher in the sealing zone than in the podosome belt (Luxenburg et al., 2007). Anyhow, whether or not the organization of a podosome belt is a prerequisite to the formation of a sealing zone still remains a matter of debate (Luxenburg et al., 2006).Therefore, podosome organization in the sealing zone may be more stable and overcome the destabilizing activity of Wrch1 that we revealed in osteoclasts plated on glass. Organization of the podosome belt and efficient bone resorption require the tyrosine kinase Pyk2, nevertheless they are independent from the

autophosphorylation of Pyk2 at Y402 (Gil-Henn et al., 2007). This suggests that Wrch1 effect on podosome belt formation was not through the inhibition of Pyk2 Y402 phosphorylation. The interference with paxillin phosphorylation may also contribute to the inhibition of podosome belt formation by Wrch1. Paxillin phosphorylation is highly dynamic during podosome belt assembly (Luxenburg et al., 2006) and it was shown to regulate invadopodia organization as cluster, ring or belt in BHK-RSV cells, resembling podosome dynamics in differentiating osteoclasts (Badowski et al., 2008). Another attractive mediator of Wrch1 effect on podosome belt assembly is Myosin II. Myosin II activity is suspected to mediate the compaction of podosomes that occurs through the contraction of the actomyosin network during osteoclast differentiation (Luxenburg et al., 2007, Saltel et al., 2004). Wrch1 and Myosin IIa present similar localization at the podosome belt (Krits et al., 2002, Ory et al., 2007) and Wrch1 was shown to be essential for myosin light chain phosphorylation that regulates Myosin II activity in epithelial cells (Chuang et al., 2007). Further studies on the role of Myosin II on the regulation of podosome organization in osteoclasts would help to elucidate the function of Wrch1 in this process.

Here, we started to solve the function of Wrch1 during osteoclastogenesis. Our data reinforce the importance of the control of osteoclast precursor adhesive and migratory properties during differentiation. Nevertheless, this aspect of osteoclast biology is poorly documented and further studies will be necessary to understand precisely the role of Wrch1 in this process. Osteoclasts have a central role in most disorders of local and systemic bone loss. The discovery of novel strategies to inhibit osteoclast activity is at present a major socioeconomic priority. Affecting small GTPase function using nitrogen containing bisphosphonates already proved very efficient to control bone loss. Nitrogen containing bisphosphonates action is to inhibit GTPase prenylation (Russell et al., 2008). Interestingly, this is not expected to affect Wrch1 activity as this atypical GTPase is palmitoylated at its

carboxyterminus, whereas most Rho family GTPases are prenylated (Berzat et al., 2005). In this regard, as this GTPase is essential for osteoclast differentiation, Wrch1/RhoU represents an interesting novel therapeutic target in view of limiting bone resorption by interfering with osteoclastogenesis.

Acknowledgments

We are very grateful to Corinne Albiges-Rizo for sharing reagents and for fruitful scientific discussion. This work was funded by institutional grants (French National Center for Scientific Research: CNRS and Montpellier I and II Universities), by the Association pour la Recherche sur le Cancer (grants 3476 and 3897) and by the Association de Recherche sur la Polyarthrite. HB and VV are recipients of fellowships from the Association pour la Recherche sur le Cancer.

References

Badowski, C., Pawlak, G., Grichine, A., Chabadel, A., Oddou, C., Jurdic, P., Pfaff, M., Albiges-Rizo, C. & Block, M. R. (2008). Paxillin Phosphorylation Controls Invadopodia/Podosomes Spatiotemporal Organization. *Mol Biol Cell, 19***,** 633-645.

Berzat, A. C., Buss, J. E., Chenette, E. J., Weinbaum, C. A., Shutes, A., Der, C. J., Minden, A. & Cox, A. D. (2005). Transforming activity of the Rho family GTPase, Wrch-1, a Wnt-regulated Cdc42 homolog, is dependent on a novel carboxyl-terminal palmitoylation motif. *J Biol Chem, 280***,** 33055-33065.

Block, M. R., Badowski, C., Millon-Fremillon, A., Bouvard, D., Bouin, A. P., Faurobert, E., Gerber-Scokaert, D., Planus, E. & Albiges-Rizo, C. (2008). Podosome-type adhesions and focal adhesions, so alike yet so different. *Eur J Cell Biol.*

Boissy, P., Machuca, I., Pfaff, M., Ficheux, D. & Jurdic, P. (1998). Aggregation of mononucleated precursors triggers cell surface expression of alphavbeta3 integrin, essential to formation of osteoclast-like multinucleated cells. *J Cell Sci, 111 (Pt 17)***,** 2563-2574.

Boyle, W. J., Simonet, W. S. & Lacey, D. L. (2003). Osteoclast differentiation and activation. *Nature, 423***,** 337-342.

Brazier, H., Stephens, S., Ory, S., Fort, P., Morrison, N. & Blangy, A. (2006). Expression profile of RhoGTPases and RhoGEFs during RANKL-stimulated osteoclastogenesis: identification of essential genes in osteoclasts. *J Bone Miner Res, 21***,** 1387-1398.

Burridge, K. & Wennerberg, K. (2004). Rho and Rac take center stage. *Cell, 116***,** 167-179.

Caswell, P. & Norman, J. (2008). Endocytic transport of integrins during cell migration and invasion. *Trends Cell Biol, 18***,** 257-263.

Cernuda-Morollon, E. & Ridley, A. J. (2006). Rho GTPases and leukocyte adhesion receptor expression and function in endothelial cells. *Circ Res, 98***,** 757-767.

Chuang, Y. Y., Valster, A., Coniglio, S. J., Backer, J. M. & Symons, M. (2007). The atypical Rho family GTPase Wrch-1 regulates focal adhesion formation and cell migration. *J Cell Sci, 120***,** 1927-1934.

Contractor, T., Babiarz, B., Kowalski, A. J., Rittling, S. R., Sorensen, E. S. & Denhardt, D. T. (2005). Osteoclasts resorb protein-free mineral (Osteologic discs) efficiently in the absence of osteopontin. *In Vivo, 19***,** 335-341.

Deakin, N. O. & Turner, C. E. (2008). Paxillin comes of age. *J Cell Sci, 121***,** 2435-2444.

Dennison, E., Cole, Z. & Cooper, C. (2005). Diagnosis and epidemiology of osteoporosis. *Curr Opin Rheumatol, 17***,** 456-461.

Destaing, O., Saltel, F., Geminard, J. C., Jurdic, P. & Bard, F. (2003). Podosomes display actin turnover and dynamic self-organization in osteoclasts expressing actin-green fluorescent protein. *Mol Biol Cell, 14***,** 407-416.

Destaing, O., Sanjay, A., Itzstein, C., Horne, W. C., Toomre, D., De Camilli, P. & Baron, R. (2008). The Tyrosine Kinase Activity of c-Src Regulates Actin Dynamics and Organization of Podosomes in Osteoclasts. *Mol Biol Cell, 19***,** 394-404.

Duong, L. T., Nakamura, I., Lakkakorpi, P. T., Lipfert, L., Bett, A. J. & Rodan, G. A. (2001). Inhibition of osteoclast function by adenovirus expressing antisense protein-tyrosine kinase 2. *J Biol Chem, 276***,** 7484-7492.

Faccio, R., Takeshita, S., Zallone, A., Ross, F. P. & Teitelbaum, S. L. (2003). c-Fms and the alphavbeta3 integrin collaborate during osteoclast differentiation. *J Clin Invest, 111***,** 749-758.

Gil-Henn, H., Destaing, O., Sims, N. A., Aoki, K., Alles, N., Neff, L., Sanjay, A., Bruzzaniti, A., De Camilli, P., Baron, R. & Schlessinger, J. (2007). Defective microtubule-dependent podosome organization in osteoclasts leads to increased bone density in Pyk2(-/-) mice. *J Cell Biol, 178***,** 1053-1064.

Humphries, J. D., Wang, P., Streuli, C., Geiger, B., Humphries, M. J. & Ballestrem, C. (2007). Vinculin controls focal adhesion formation by direct interactions with talin and actin. *J Cell Biol, 179***,** 1043-1057.

Jurdic, P., Saltel, F., Chabadel, A. & Destaing, O. (2006). Podosome and sealing zone: specificity of the osteoclast model. *Eur J Cell Biol, 85***,** 195-202.

Kim, J. M., Min, S. K., Kim, H., Kang, H. K., Jung, S. Y., Lee, S. H., Choi, Y., Roh, S., Jeong, D. & Min, B. M. (2007). Vacuolar-type H+-ATPase-mediated acidosis promotes in vitro osteoclastogenesis via modulation of cell migration. *Int J Mol Med, 19***,** 393-400.

Kim, K., Lee, S. H., Ha Kim, J., Choi, Y. & Kim, N. (2008). NFATc1 Induces Osteoclast Fusion Via Up-Regulation of Atp6v0d2 and the Dendritic Cell-Specific Transmembrane Protein (DC-STAMP). *Mol Endocrinol, 22***,** 176-185.

Krits, I., Wysolmerski, R. B., Holliday, L. S. & Lee, B. S. (2002). Differential localization of myosin II isoforms in resting and activated osteoclasts. *Calcif Tissue Int, 71***,** 530-538.

Lakkakorpi, P. T., Bett, A. J., Lipfert, L., Rodan, G. A. & Duong le, T. (2003). PYK2 autophosphorylation, but not kinase activity, is necessary for adhesion-induced association with c-Src, osteoclast spreading, and bone resorption. *J Biol Chem, 278***,** 11502-11512.

Lee, S. H., Rho, J., Jeong, D., Sul, J. Y., Kim, T., Kim, N., Kang, J. S., Miyamoto, T., Suda, T., Lee, S. K., Pignolo, R. J., Koczon-Jaremko, B., Lorenzo, J. & Choi, Y. (2006). v-ATPase V0 subunit d2-deficient mice exhibit impaired osteoclast fusion and increased bone formation. *Nat Med, 12***,** 1403-1409.

Luxenburg, C., Addadi, L. & Geiger, B. (2006). The molecular dynamics of osteoclast adhesions. *Eur J Cell Biol, 85***,** 203-211.

Luxenburg, C., Geblinger, D., Klein, E., Anderson, K., Hanein, D., Geiger, B. & Addadi, L. (2007). The architecture of the adhesive apparatus of cultured osteoclasts: from podosome formation to sealing zone assembly. *PLoS ONE, 2***,** e179.

McHugh, K. P., Hodivala-Dilke, K., Zheng, M. H., Namba, N., Lam, J., Novack, D., Feng, X., Ross, F. P., Hynes, R. O. & Teitelbaum, S. L. (2000). Mice lacking beta3 integrins are osteosclerotic because of dysfunctional osteoclasts. *J Clin Invest, 105***,** 433-440.

Miyamoto, T., Arai, F., Ohneda, O., Takagi, K., Anderson, D. M. & Suda, T. (2000). An adherent condition is required for formation of multinuclear osteoclasts in the presence of macrophage colony-stimulating factor and receptor activator of nuclear factor kappa B ligand. *Blood, 96***,** 4335-4343.

Miyazaki, T., Sanjay, A., Neff, L., Tanaka, S., Horne, W. C. & Baron, R. (2004). Src kinase activity is essential for osteoclast function. *J Biol Chem, 279***,** 17660-17666.

Nakamura, I., Lipfert, L., Rodan, G. A. & Le, T. D. (2001). Convergence of alpha(v)beta(3) integrin- and macrophage colony stimulating factor-mediated signals on phospholipase Cgamma in prefusion osteoclasts. *J Cell Biol, 152***,** 361-373.

Ogasawara, T., Katagiri, M., Yamamoto, A., Hoshi, K., Takato, T., Nakamura, K., Tanaka, S., Okayama, H. & Kawaguchi, H. (2004). Osteoclast differentiation by RANKL requires NF-kappaB-mediated downregulation of cyclin-dependent kinase 6 (Cdk6). *J Bone Miner Res, 19***,** 1128-1136.

Ory, S., Brazier, H. & Blangy, A. (2007). Identification of a bipartite focal adhesion localization signal in RhoU/Wrch-1, a Rho family GTPase that regulates cell adhesion and migration. *Biol Cell, 99***,** 701-716.

Ory, S., Brazier, H., Pawlak, G. & Blangy, A. (2008). Rho GTPases in osteoclasts: Orchestrators of podosome arrangement. *Eur J Cell Biol, 87***,** 469-477.

Ory, S., Munari-Silem, Y., Fort, P. & Jurdic, P. (2000). Rho and Rac exert antagonistic functions on spreading of macrophage-derived multinucleated cells and are not required for actin fiber formation. *J Cell Sci, 113 (Pt 7)*, 1177-1188.

Roodman, G. D. (2006). Regulation of osteoclast differentiation. *Ann N Y Acad Sci, 1068*, 100-109.

Russell, R. G., Watts, N. B., Ebetino, F. H. & Rogers, M. J. (2008). Mechanisms of action of bisphosphonates: similarities and differences and their potential influence on clinical efficacy. *Osteoporos Int*.

Ruusala, A. & Aspenstrom, P. (2008). The atypical Rho GTPase Wrch1 collaborates with the nonreceptor tyrosine kinases Pyk2 and Src in regulating cytoskeletal dynamics. *Mol Cell Biol, 28*, 1802-1814.

Saltel, F., Chabadel, A., Bonnelye, E. & Jurdic, P. (2008). Actin cytoskeletal organisation in osteoclasts: A model to decipher transmigration and matrix degradation. *Eur J Cell Biol*.

Saltel, F., Destaing, O., Bard, F., Eichert, D. & Jurdic, P. (2004). Apatite-mediated actin dynamics in resorbing osteoclasts. *Mol Biol Cell, 15*, 5231-5241.

Sanjay, A., Houghton, A., Neff, L., DiDomenico, E., Bardelay, C., Antoine, E., Levy, J., Gailit, J., Bowtell, D., Horne, W. C. & Baron, R. (2001). Cbl associates with Pyk2 and Src to regulate Src kinase activity, alpha(v)beta(3) integrin-mediated signaling, cell adhesion, and osteoclast motility. *J Cell Biol, 152*, 181-195.

Saras, J., Wollberg, P. & Aspenstrom, P. (2004). Wrch1 is a GTPase-deficient Cdc42-like protein with unusual binding characteristics and cellular effects. *Exp Cell Res, 299*, 356-369.

Shutes, A., Berzat, A. C., Cox, A. D. & Der, C. J. (2004). Atypical mechanism of regulation of the Wrch-1 Rho family small GTPase. *Curr Biol, 14*, 2052-2056.

Shyu, J. F., Shih, C., Tseng, C. Y., Lin, C. H., Sun, D. T., Liu, H. T., Tsung, H. C., Chen, T. H. & Lu, R. B. (2007). Calcitonin induces podosome disassembly and detachment of osteoclasts by modulating Pyk2 and Src activities. *Bone, 40***,** 1329-1342.

Takayanagi, H., Kim, S., Koga, T., Nishina, H., Isshiki, M., Yoshida, H., Saiura, A., Isobe, M., Yokochi, T., Inoue, J., Wagner, E. F., Mak, T. W., Kodama, T. & Taniguchi, T. (2002). Induction and activation of the transcription factor NFATc1 (NFAT2) integrate RANKL signaling in terminal differentiation of osteoclasts. *Dev Cell, 3***,** 889-901.

Teitelbaum, S. L. & Ross, F. P. (2003). Genetic regulation of osteoclast development and function. *Nat Rev Genet, 4***,** 638-649.

Wang, Y., Lebowitz, D., Sun, C., Thang, H., Grynpas, M. D. & Glogauer, M. (2008). Identifying the relative contributions of rac1 and rac2 to osteoclastogenesis. *J Bone Miner Res, 23***,** 260-270.

Webb, D. J., Donais, K., Whitmore, L. A., Thomas, S. M., Turner, C. E., Parsons, J. T. & Horwitz, A. F. (2004). FAK-Src signalling through paxillin, ERK and MLCK regulates adhesion disassembly. *Nat Cell Biol, 6***,** 154-161.

Webb, D. J., Parsons, J. T. & Horwitz, A. F. (2002). Adhesion assembly, disassembly and turnover in migrating cells -- over and over and over again. *Nat Cell Biol, 4***,** E97-100.

Zhang, X. A. & Hemler, M. E. (1999). Interaction of the integrin beta1 cytoplasmic domain with ICAP-1 protein. *J Biol Chem, 274***,** 11-19.

Zou, W., Kitaura, H., Reeve, J., Long, F., Tybulewicz, V. L., Shattil, S. J., Ginsberg, M. H., Ross, F. P. & Teitelbaum, S. L. (2007). Syk, c-Src, the alphavbeta3 integrin, and ITAM immunoreceptors, in concert, regulate osteoclastic bone resorption. *J Cell Biol, 176***,** 877-888.

Figure Legends

Figure 1: Wrch1 protein expression is induced during osteoclastogenesis.

(A) RAW264.7 cells were grown for the indicated periods of time in differentiation medium. Total protein extracts were prepared and analyzed by western blot using purified anti-Wrch1 and anti-Gapdh antibodies. (B) Intensity of the bands in (A) was quantified using ImageJ. (A) and (B) are representative of three independent experiments. (C) Immunoblotting of protein lysates from shLucif and shWrch1 RAW264.7 cells grown for 0 or 5 days in the presence of RANKL, using anti-Wrch1 and anti-Gapdh antibodies. (D) Analysis of the expression of osteoclast specific markers in RAW264.7 cells treated for 0 (black bars) and 3 days (white bars) with 25 ng/ml RANKL. All bar graphs show the cDNA levels of the indicated genes relative to Gapdh in the same sample, determined by quantitative PCR. Error bars: 95% confidence limits of the Gene/Gapdh ratios. All graphs are representative of at least two independent experiments. (E) RAW264.7 cells stably expressing GFP or GFP-fused Wrch1 wild type (Wrch1-WT) or active mutant (Wrch1-Q107L) were cultured in growth medium and cell numbers were measured after 1, 2, 3 and 4 days. Shown is the average and standard deviation of 3 wells from one experiment representative of two.

Figure 2: Wrch1 induces RAW264.7 cell aggregation and rounding.

(A) RAW264.7 cells expressing GFP of GFP-fused Wrch1-WT or -Q107L were seeded on tissue culture plates and grown in the presence (+RANKL) of absence (-RANKL) of 50 ng/ml RANKL. Photos shown are representative of each condition after 3 days of culture (10X objective). (B) The same cells were scraped, dissociated and submitted to an aggregation test in suspension, in the presence of EDTA to prevent or Ca2+ to allow cell-cell contact reformation. After 15 minutes of treatment, representative photographs of each

condition were taken using a 20X objective. (C) RAW264.7 cells stably expressing GFP or GFP-fused Wrch1-WT or -Q107L were seeded on tissue culture plates for 48 hours and the proportion of spread cells was determined for each conditions. Photos taken with a 40X objective are representative of each condition. Bar graph shows average and standard deviations of the proportions of spread cells from 3 independent experiments.

Figure 3: Wrch1 inhibits RAW264.7 cell adhesion onto vitronectin and integrin αvß3 signaling.

(A) Undifferentiated RAW264.7 cells stably expressing GFP (GFP, empty boxes) or GFP-fused Wrch1-WT (WT, triangles) or -Q107L (Q107L, crosses) or preOCLs expressing GFP (GFP+RANKL, diamonds) were submitted to an adhesion test onto vitronectin for 30 minutes. The proportion of adherent cells was then determined for each concentration of vitronectin. (B) Same experiment as in (A) performed onto fibronectin. (C) Bone marrow macrophages expressing GFP (GFP, diamonds) or GFP-fused Wrch1-Q107L (Q107L, boxes) or BMM derived preOCLs expressing GFP (GFP+RANKL, triangles) were submitted to an adhesion test onto vitronectin for 45 minutes. The proportion of adherent cells was then determined for each concentration of vitronectin. Graphs in A, B and C show average and standard deviations of the percentage of attached cells relative to the number of seeded cells and are representative of 4 (A and B) or 3 (C) independent experiments performed in triplicates. (D) Total cell extracts were prepared from undifferentiated RAW264.7 cells expressing GFP or GFP fused Wrch1-Q107L after the indicated time of adhesion on vitronectin. Protein phosphorylation was analyzed by western blot using the indicated antibodies. The experiment shown is representative of 2 experiments. (E) Lysates from HEK293T cells expressing GFP or GFP-fused Wrch1-WT (WT) or Wrch1-Q107L (Q107L) were incubated with GST or GST-fused integrin ß3 cytoplasmic domain (ß3) bound to

Glutathionne-S-Sepharose beads. Proteins in cell lysates (TCL) and bound to the beads (pull down) were analyzed by western blot unsing anti-GFP antibodies. (F) Lysates from RAW264.7 cells expressing GFP or GFP-fused Wrch1-Q107L (Q107L) were treated as in (D). Proteins in cell lysates (TCL) and bound to the beads (pull down) were analyzed by western blot using anti-GFP and anti-Pyk2 antibodies.

Figure 4: Wrch1 interferes with preosteoclast chemotactic migration.

(A) 5000 undifferentiated RAW264.7 cells (- RANKL, white bars) or preosteoclasts (+RANKL, grey bars), stably expressing GFP (c) or GFP-fused Wrch1-WT (WT) or -Q107L (Q), were submitted to a transwell migration test for 24 hours in the absence (- MCSF) or presence (+ MCSF) of 50 ng/ml M-CSF in the lower chambers. (B) 5000 undifferentiated BMMs (- RANKL, white bars) or BMM-derived preosteoclasts (+RANKL, grey bars), stably expressing GFP (c) or GFP-fused Wrch1-Q107L (Q), were submitted to a transwell migration test for 24 hours in the presence of 10 ng/mL (- MCSF) or 60 ng/mL M-CSF (+ MCSF) in the lower chambers. Bar graphs shows average and standard deviation of the proportions of cells that had migrated to the lower chamber, calculated from 2 independent experiments performed in duplicates. **: significant difference, $p<0,01$ as determined by Mann and Whitney non-parametric statistic test. (C) Similar experiment as in (A) was performed on RAW264.7 derived preosteoclasts expressing shRNAs against Firefly Luciferase (c) or Wrch1 (shW), in the absence (black bars) or presence (dashed bars) of 50 ng/mL M-CSF in the lower chambers. Bar graphs in A and B show average and standard deviation of the proportions of cells that had migrated to the lower chamber, calculated from 3 independent experiments performed in duplicates. **: significant difference, $p<0,01$ as determined by Kruskal and Wallis non-parametric statistic test. (D) Efficiency of Wrch1 silencing in preosteoclasts: total protein extracts, prepared from RAW264.7 cells expressing shRNAs

against Firefly Luciferase (shLuc) or Wrch1 (shWrch) and treated for 0 or 3 days with RANKL, were analyzed by western blot using purified anti-Wrch1 and anti-Actin antibodies. This western blot is representative of cells used in the migration experiments described in (B).

Figure 5: Wrch1 affects podosome organization in osteoclasts.

(A) Osteoclasts differentiated from RAW264.7 cells stably expressing GFP, or GFP fused Wrch1-WT (WT), Wrch1-Q107L (Q107L) or Wrch1-T63N (T63N) were fixed and actin was labeled using rhodamine-phalloidine to determine the organization of podosomes as clusters and rings (grey bars) or belts (white bars), as illustrated by fluorescent microscope images. Bar graph shows the average and standard deviations of the proportions of osteoclasts in each category, calculated from three independent experiment and counting at least 1000 osteoclasts per condition and per experiment. (B) The same osteoclasts expressing GFP fused wild type (WT), active (Q107L) or inactive (T63N) Wrch1 were seeded on Osteologic calcium-phosphate coated coverslips for 48 hours, fixed and labeled for actin and vinculin. Individual deconvolved 300 nm optical slices are shown. GFP (green) and Vinculin (red) staining were overlayed in right panels. Insets show enlarged boxed areas. (C) The same osteoclasts were seeded in Osteologic calcium-phosphate coated wells. After 48 hours, mineralized matrix was stained by Von Kossa to measure resorbed areas. Bar graph shows the average and standard deviations of the total surface resorbed per osteoclast, calculated from two independent experiments performed in triplicates.

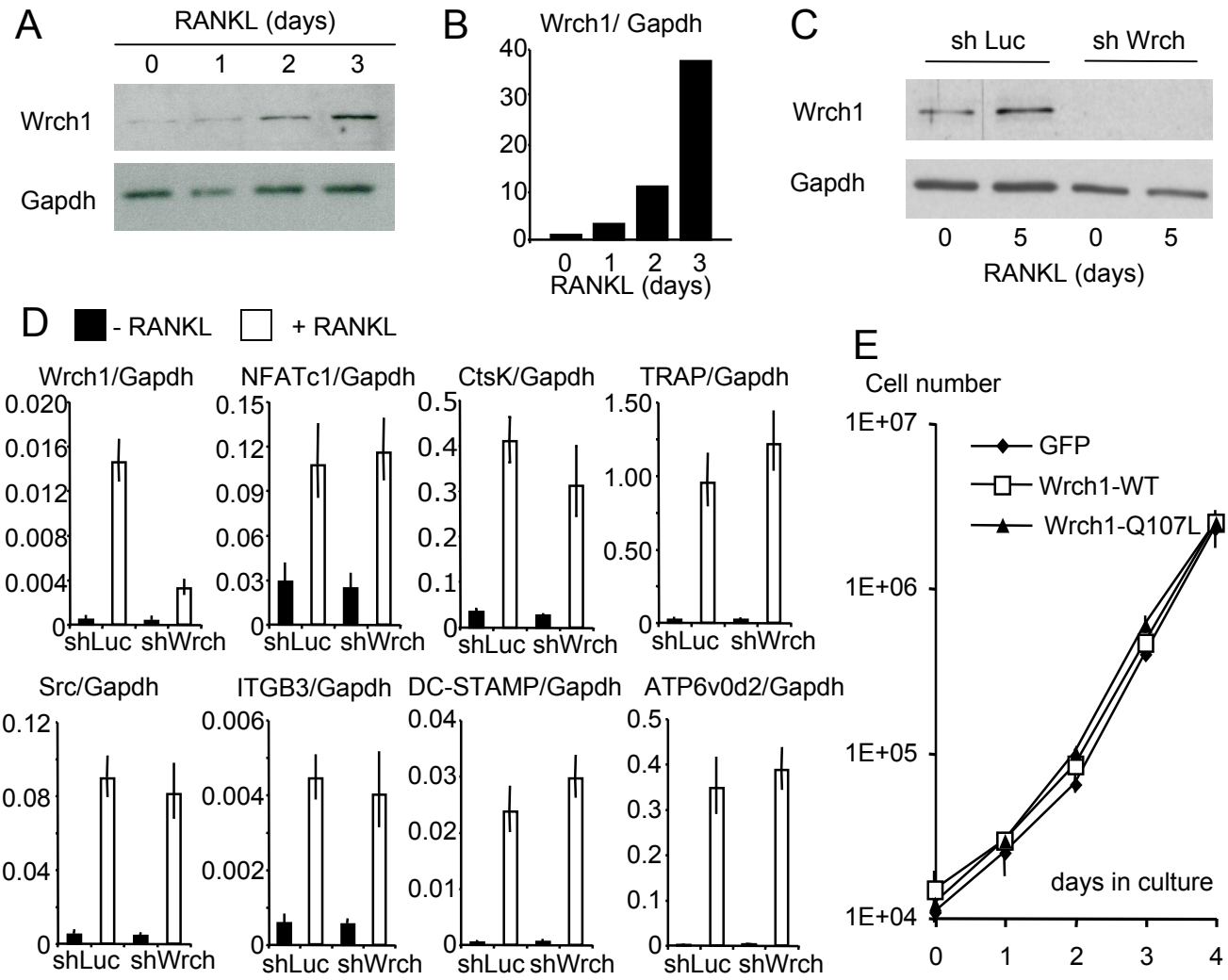

Brazier et al. Fig1

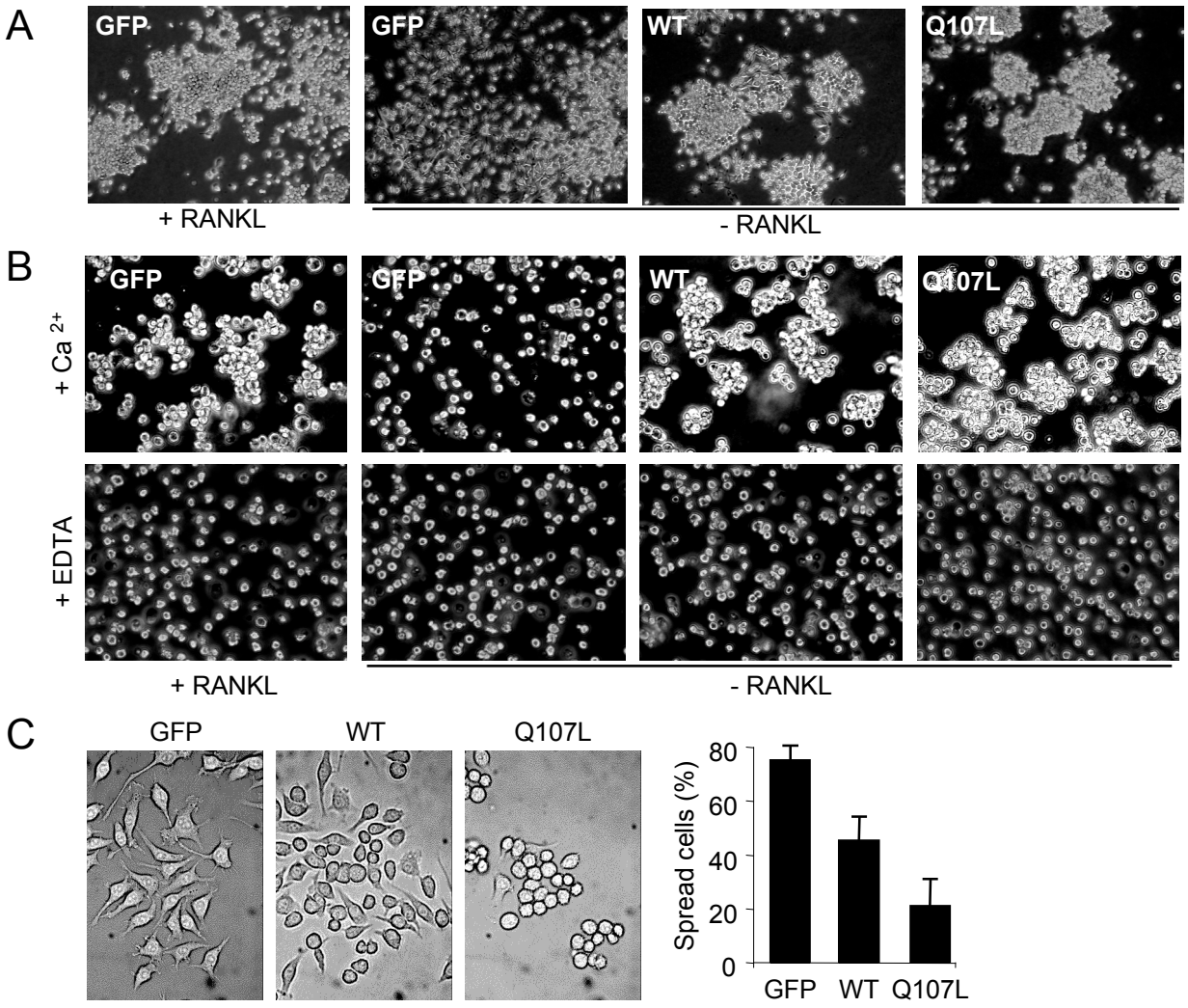

Brazier et al. Fig2

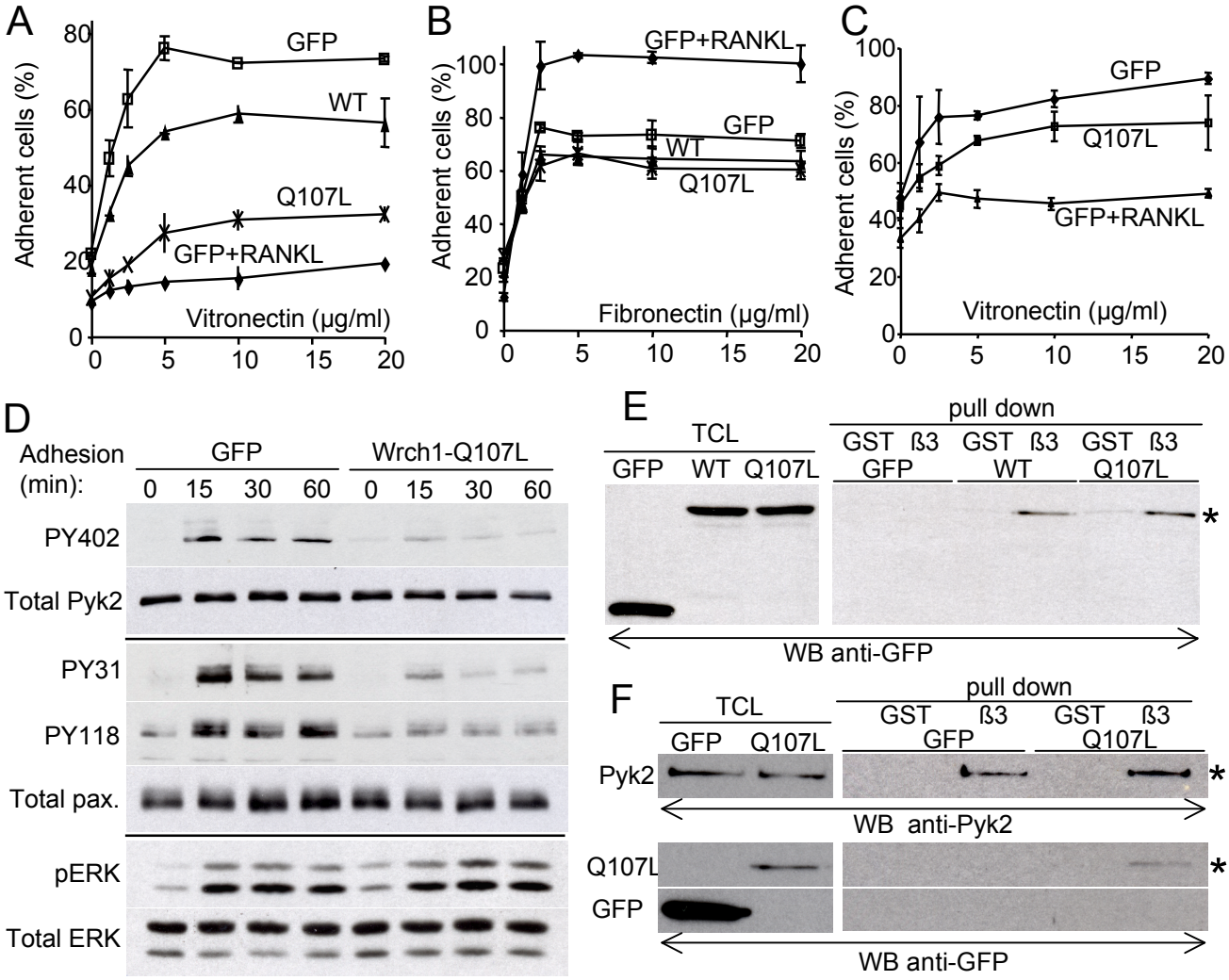

Brazier et al. Fig3

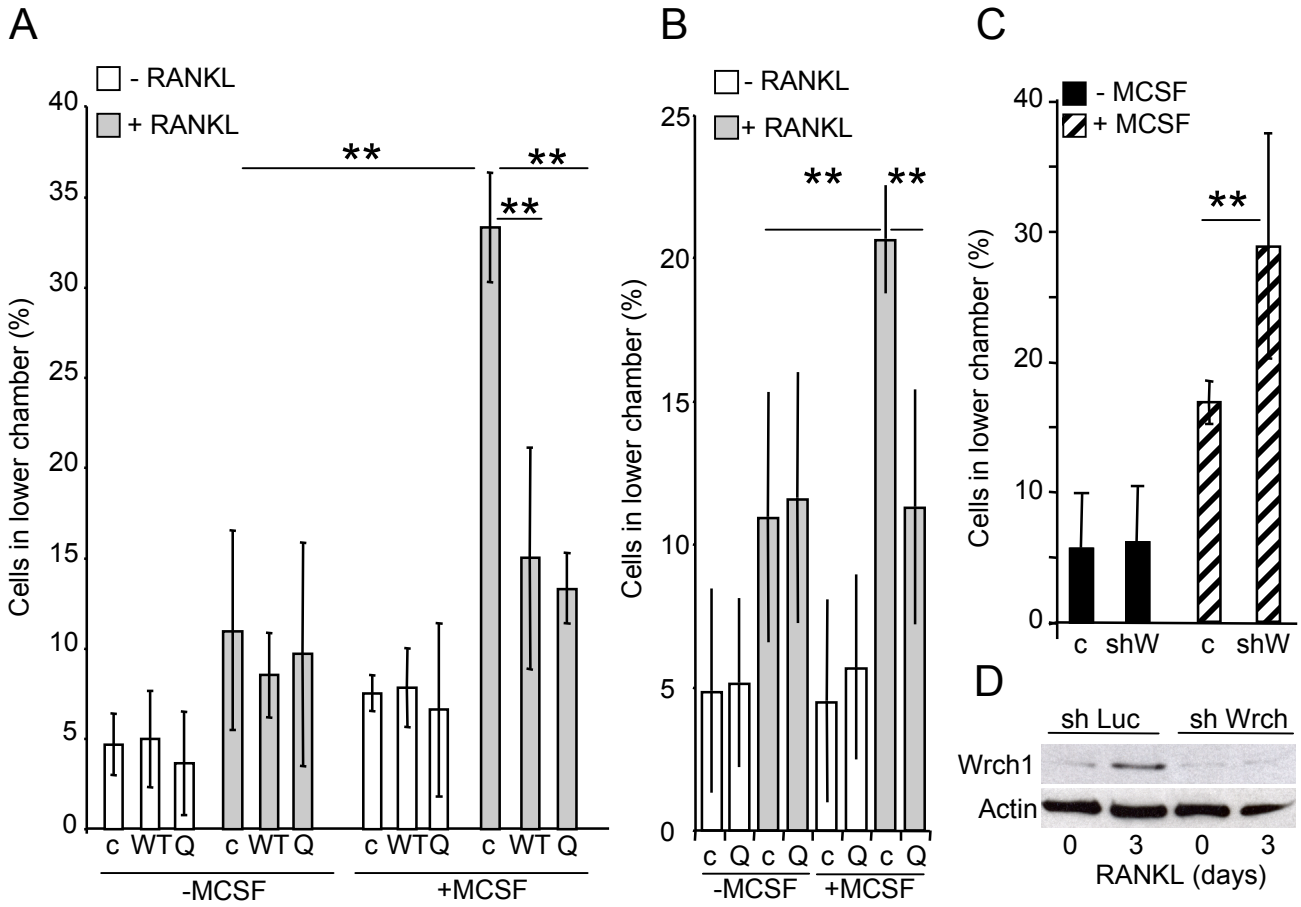

Brazier et al. Fig4

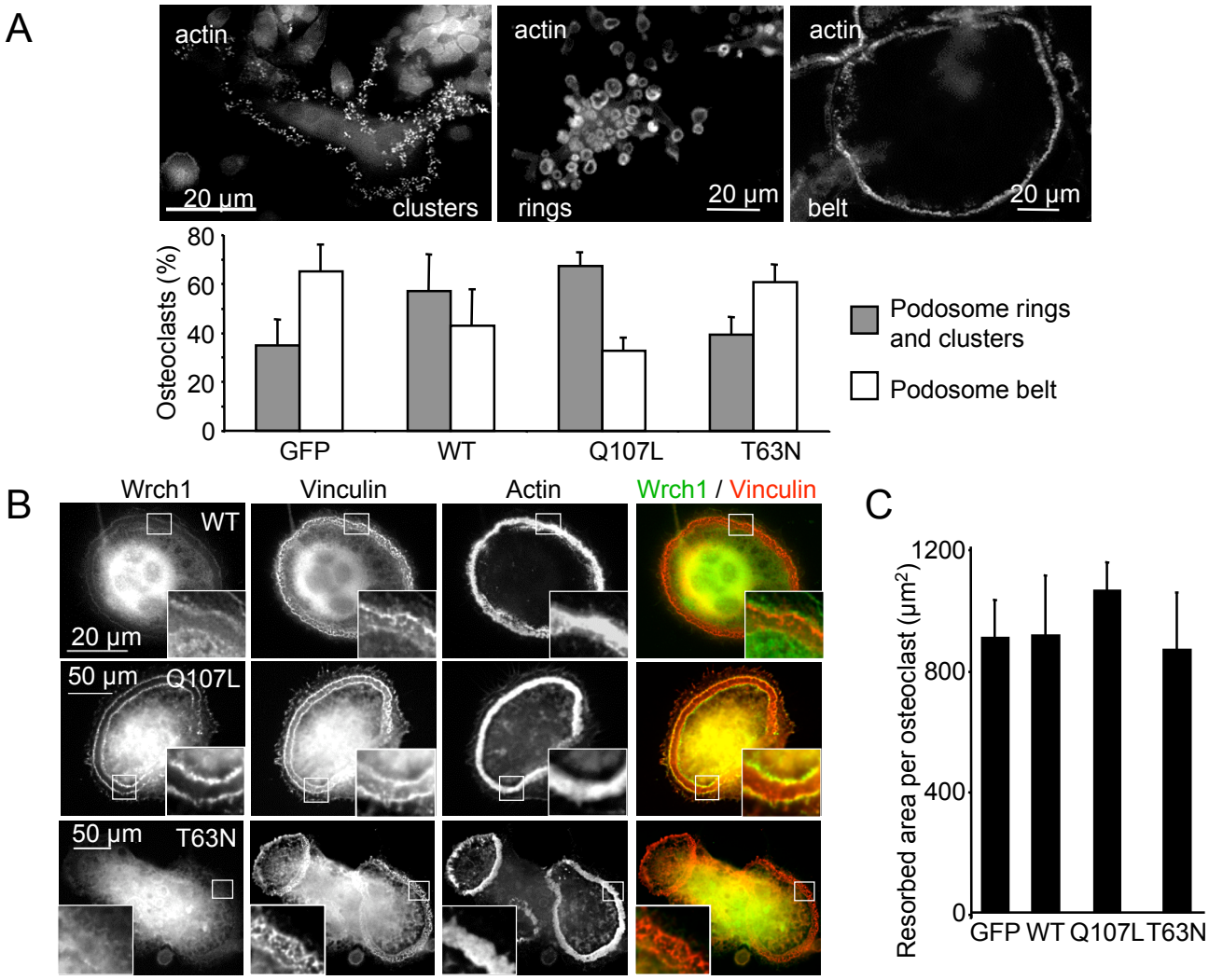

Brazier et al. Fig 5